

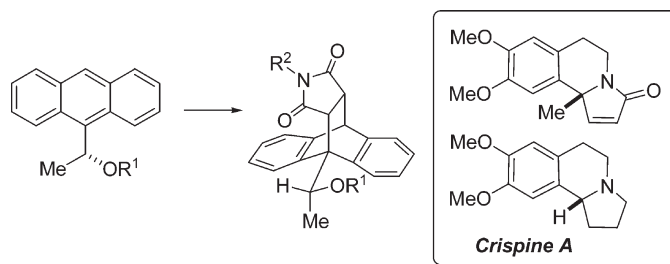
## Diastereoselective Cycloadditions and Transformations of *N*-Alkyl and *N*-Aryl Maleimides with Chiral 9-Anthrylethanol Derivatives

Harry Adams, Tareg M. Elsunaki, Isaac Ojea-Jiménez, Simon Jones,\* and Anthony J. H. M. Meijer

Department of Chemistry, Dainton Building, University of Sheffield, Brook Hill, Sheffield S3 7HF, U.K.

simon.jones@sheffield.ac.uk

Received July 22, 2010



Thermal Diels–Alder reactions of chiral 9-methoxyethyl and 9-hydroxyethyl anthracene have been investigated both experimentally and computationally with a range of *N*-substituted maleimides. Whereas cycloadditions with 9-methoxyethyl anthracene proceeded with almost complete diastereoselectivity, those with 1-anthracene-9-yl-ethanol resulted in essentially no diastereoselectivity. Subsequent regio- and stereoselective transformations with reducing agents and carbon nucleophiles demonstrated the synthetic utility of this methodology, which was applied to the enantioselective synthesis of pyrrolo[2,1-*a*]isoquinolines and an attempted synthesis of the alkaloid crispine A. Computational studies supported the proposed hypotheses for the stereoselectivity observed in the transformations described.

### Introduction

Chiral auxiliary approaches are well established for the preparation of enantioenriched building blocks in academic and industrial environments worldwide. Although auxiliaries based upon acyl group functionalization are well established, there have been fewer reports on synthetic manipulations that may be carried out using chiral diene auxiliaries, where the attachment and cleavage steps proceed through Diels–Alder and retro-Diels–Alder steps, respectively. Although chiral cyclopentadienes have been successfully

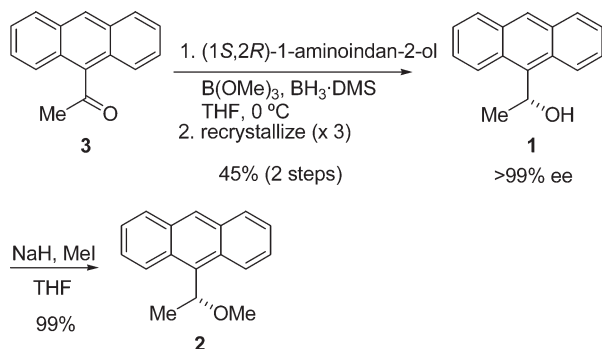
employed as stereocontrolling elements in this manner,<sup>1</sup> more recently, studies independently conducted by Snyder<sup>2</sup> and this group<sup>3</sup> have championed the use of chiral anthracene templates, one of the primary advantages being the elimination of the possibility of *endo* and *exo* isomers in the initial Diels–Alder addition step. Much of the early work conducted by ourselves and Snyder focused on the use of maleimides as benchmark substrates to evaluate reactivity and selectivity. Notably, we observed that 9-(1-hydroxyethyl)-anthracene led to enhanced reactivity, but reduced selectivity with such dienophiles, and proposed that this was due to hydrogen bonding effects overriding the inherent electron

(1) (a) Riviere, P.; Mauvais, A.; Winterfeldt, E. *Tetrahedron: Asymmetry* **1994**, *5*, 1831–1846. (b) Beil, W.; Jones, P. G.; Nerenz, F.; Winterfeldt, E. *Tetrahedron* **1998**, *54*, 7273–7292. (c) Gerstenberger, I.; Hansen, M.; Mauvais, A.; Wartchow, R.; Winterfeldt, E. *Eur. J. Org. Chem.* **1998**, 643–650.

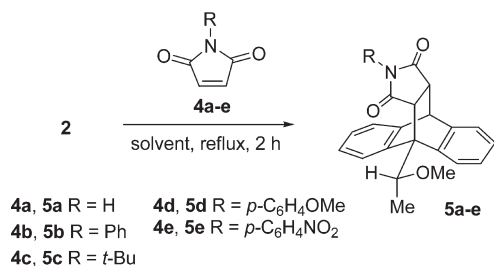
(2) (a) Sanyal, A.; Snyder, J. K. *Org. Lett.* **2000**, *2*, 2527–2530. (b) Corbett, M. S.; Liu, X.; Sanyal, A.; Snyder, J. K. *Tetrahedron Lett.* **2003**, *44*, 931–935. (c) Burgess, K. L.; Corbett, M. S.; Eugenio, P.; Lajkiewicz, N. J.; Liu, X.; Sanyal, A.; Yan, W.; Yuan, Q.; Snyder, J. K. *Bioorg. Med. Chem.* **2005**, *13*, 5299–5309. (d) Burgess, K. L.; Lajkiewicz, N. J.; Sanyal, A.; Yan, W.; Snyder, J. K. *Org. Lett.* **2005**, *7*, 31–34. (e) Sanyal, A.; Yuan, Q.; Snyder, J. K. *Tetrahedron Lett.* **2005**, *46*, 2475–2478. (f) Liu, X.; Snyder, J. K. *J. Org. Chem.* **2008**, *73*, 2935–2938.

(3) (a) Atherton, J. C. C.; Jones, S. *Tetrahedron Lett.* **2001**, *42*, 8239–8241. (b) Jones, S.; Atherton, J. C. C. *Tetrahedron: Asymmetry* **2001**, *12*, 1117–1119. (c) Atherton, J. C. C.; Jones, S. *Tetrahedron Lett.* **2002**, *43*, 9097–9100. (d) Atherton, J. C. C.; Jones, S. *J. Chem. Soc., Perkin Trans. 1* **2002**, 2166–2173. (e) Bawa, R. A.; Jones, S. *Tetrahedron* **2004**, *60*, 2765–2770. (f) Jones, S.; Ojea-Jimenez, I. *Polycyclic Aromat. Compd.* **2005**, *25*, 1–12. (g) Adams, H.; Bawa, R. A.; Jones, S. *Org. Biomol. Chem.* **2006**, *4*, 4206–4213. (h) Adams, H.; Jones, S.; Ojea-Jimenez, I. *Org. Biomol. Chem.* **2006**, *4*, 2296–2303. (i) Adams, H.; Bawa, R. A.; McMillan, K. G.; Jones, S. *Tetrahedron: Asymmetry* **2007**, *18*, 1003–1012.

## SCHEME 1. Synthesis of Chiral Dienes



## SCHEME 2. Diels–Alder Reaction of Ether 2



pair repulsion responsible for the excellent levels of diastereoselectivity usually observed. Snyder's group went on to functionalize *N*-methyl, *N*-allyl and *N*-homoallyl maleimide cycloadducts of 9-(1,2-dimethoxyethyl)anthracene and 9-( $\alpha$ -methylbenzylamine)anthracene using Grignard and hydride reducing agents in a high regio- and stereoselective manner. We were interested in further exploring the chemistry of the maleimide substrates, in particular looking at the effect of the size and electronic nature of the *N*-substituent upon on the diastereoselectivity with both 9-(1-methoxyethyl)anthracene and 9-(1-hydroxyethyl)anthracene, and then examining whether the functionalization protocols described by Snyder were applicable to some of the 9-(1-methoxyethyl)anthracene frameworks.

## Results and Discussion

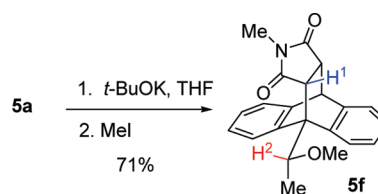
The initial target auxiliaries 9-(1-hydroxyethyl)anthracene **1** and 9-(1-methoxyethyl)anthracene **2** were prepared in racemic form using a reported procedure.<sup>3d</sup> The enantiomerically enriched version of the carbinol (*R*)-**2** was prepared in a 78% ee *via* modification of a previous procedure by asymmetric reduction of the ketone **3** in the presence of catalytic amounts of the oxazaborolidine derived from (1*S*,2*R*)-1-aminoindan-2-ol (Scheme 1). Repeated recrystallization of the crude material from dichloromethane and petroleum ether (40–60 °C) afforded the desired alcohol (*R*)-**2** in 45% yield and >99% enantiomeric excess (by HPLC), whose absolute configuration was determined by comparison of the specific rotation with the literature value. The (*R*)-carbinol **2** obtained was converted into (*R*)-9-(1-methoxyethyl)anthracene **1** following the reported procedure.<sup>3d</sup> Likewise, (*S*)-9-(1-methoxyethyl)anthracene **1** could be obtained by an identical procedure employing (1*S*,2*R*)-1-aminoindan-2-ol as catalyst precursor.

The thermal Diels–Alder reactions of maleimides **4a–e** with the methyl ether (*R*)-**2** were carried out by heating the

TABLE 1. Thermal Diels–Alder Additions of the Methyl Ether **2** with Maleimides **4a–e**<sup>a</sup>

entry	imide	solvent	conv (%) <sup>b</sup>	de (%) <sup>b</sup>	yield (%) <sup>c</sup>
1	<b>4a</b>	CH <sub>2</sub> Cl <sub>2</sub>	>95	>95	86
2	<b>4a</b>	toluene	>95	>95	
3	<b>4b</b>	CH <sub>2</sub> Cl <sub>2</sub>	>95	>95	87
4	<b>4b</b>	toluene	>95	>95	
5	<b>4c</b>	CH <sub>2</sub> Cl <sub>2</sub>	22	>95	
6	<b>4c</b>	toluene	>95	>95	81
7	<b>4d</b>	CH <sub>2</sub> Cl <sub>2</sub>	>95	>95	95
8	<b>4d</b>	toluene	>95	>95	
9	<b>4e</b>	CH <sub>2</sub> Cl <sub>2</sub>	>95	>95	92
10	<b>4e</b>	toluene	>95	>95	

<sup>a</sup>Reactions performed by heating ether **2** (1.7 mmol) and dienophile (1.7 mmol) in dry degassed solvent (15 mL) at reflux for 2 h, followed by evaporation of the solvent. <sup>b</sup>Calculated from the ratios of the integrals corresponding to appropriate signals in the <sup>1</sup>H NMR spectrum of the crude reaction mixture. <sup>c</sup>Based on isolated product.

SCHEME 3. Methylation of Cycloadduct **5a**

reactants at reflux in dry degassed CH<sub>2</sub>Cl<sub>2</sub> and/or toluene for 2 h (Scheme 2). Apart from the reaction of the *tert*-butylmaleimide **4c**, almost complete conversion was observed as determined by comparison of the starting material and product peaks in the <sup>1</sup>H NMR spectrum (Table 1). For the *tert*-butylmaleimide **4c**, a low conversion of 22% in CH<sub>2</sub>Cl<sub>2</sub> was observed (entry 5, Table 1). However, if the temperature of the reaction was increased by changing the solvent to toluene, the amount of product obtained was seen to rise (entry 6, Table 1). This lower reactivity most likely results from an increased activation energy resulting from increased steric interactions between the *tert*-butyl group and the anthracene ring system. As expected all reactions produced exclusively the addition adducts **5a–e** as single diastereoisomers (*vide infra*), which after recrystallization from CH<sub>2</sub>Cl<sub>2</sub>/petrol 60–80 °C were isolated in high yields ranging from 81% to 95% (Table 1).

The relative stereochemistry of the addition product **5b** was confirmed by single crystal X-ray diffraction. The orientation of the methyl group antiperiplanar to the ring system and the methoxy substituent away from the carbonyl group proximal to the C-9 position agrees with previous elucidated crystal structures corresponding to the maleic anhydride and *N*-methylmaleimide analogues.<sup>3d</sup> Of particular interest is the *N*-phenyl substituent that adopts a conformation perpendicular to the underlying anthracene aromatic system to minimize steric repulsion with adjacent carbonyl groups. This conformation was also adopted in solution indicated by the observation in the <sup>1</sup>H NMR spectrum of two of the signals corresponding to aromatic protons of the *N*-phenyl substituent shifted to 6.50 ppm (as compared to the rest being in the region of 7.22–7.94 ppm) due to an anisotropic effect. The identity of the addition product **5a** was confirmed by *N*-methylation using potassium *tert*-butoxide and methyl iodide (Scheme 3) and comparison of <sup>1</sup>H NMR data of the product **5f** with that of previously reported compounds of known stereochemistry.<sup>3d</sup>

The identity of cycloadducts **5c–e** was further confirmed by correlation of selected signals from the  $^1\text{H}$  NMR spectrum of known addition product **5f** with the diastereoisomers **5a–e**.

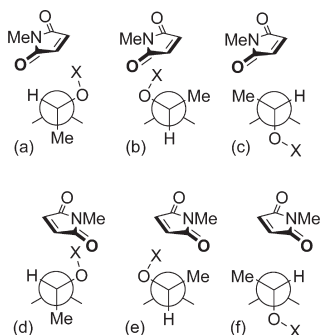


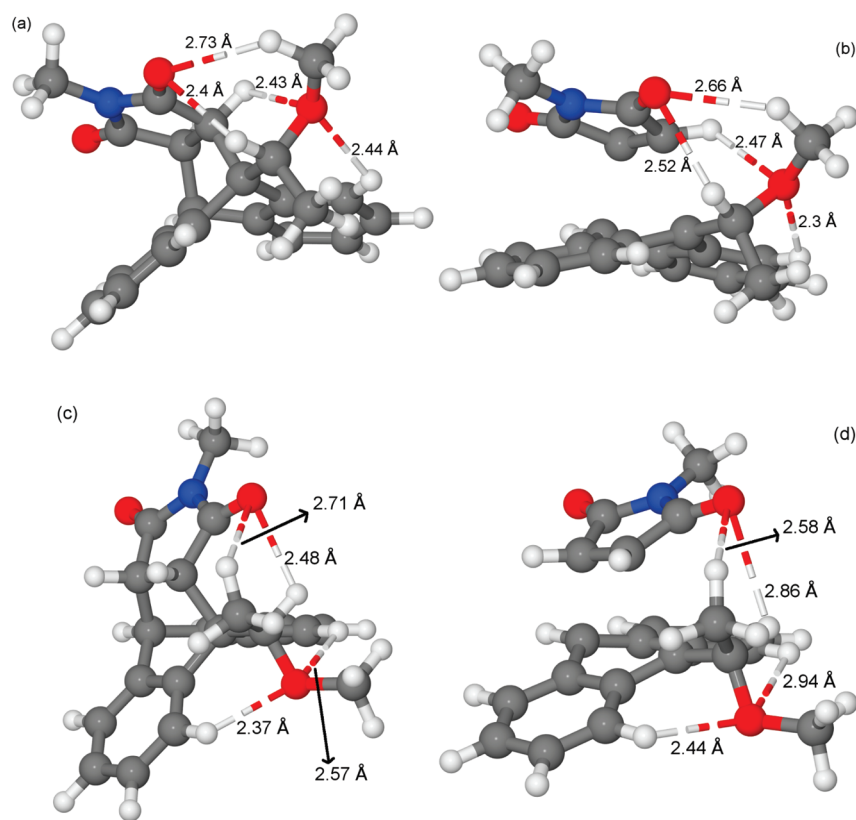
**FIGURE 1.** Six different possible geometries for the Diels–Alder reaction of anthracene derivative **2** with *N*-methyl maleimide (X = Me, H).

**TABLE 2.** Gibbs Energy of Formation and Gibbs Energy of Activation Compared to Reactants at Infinite Separation for the 6 Reaction Geometries Depicted in Figure 1 (X = Me)

reaction geometry	Gibbs energy of activation (kJ/mol)	Gibbs energy of reaction (kJ/mol)
(a)	137.46	3.55
(b)	176.16	25.39
(c)	162.09	30.73
(d)	155.23	28.823
(e)	188.27	43.90
(f)	153.28	4.33

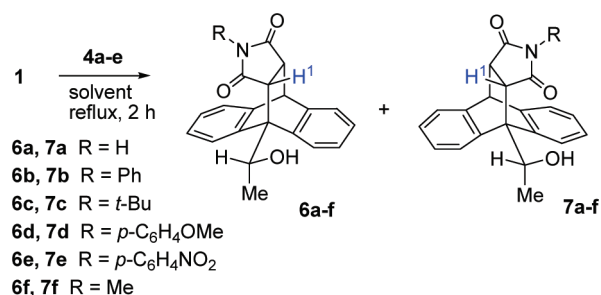
These results are then in accordance with the model proposed by Snyder,<sup>2a</sup> where formation of the *syn*-diastereoisomer is not favorable because of electrostatic repulsion between the methoxy substituent and the carbonyl group in the transition state. However, to put this observation on a firmer footing, we performed a series of density functional theory (DFT) calculations for the formation of imide **5f**. Here there are 6 different possible reaction geometries, similar to those proposed in the case of the reaction with maleic anhydride (Figure 1, X = Me).<sup>4</sup> For each of these, the Gibbs energy of formation from reactants and the Gibbs energy for the transition state were calculated (Table 2).

It is clear that geometries (a) and (f) lead to the lowest energy structures and that of these geometry (a) has a significantly lower Gibbs energy of activation, which is also the lowest of the six reaction geometries under consideration. From the plots of these minimum energy and transition state structures (Figure 2) it is apparent that there are a number of attractive interactions that clearly stabilize these geometries. In particular, there is a strong van der Waals interaction between the lone hydrogen on the auxiliary ligand and the carbonyl oxygen of the maleimide in both cases. In the case of the favored reaction geometry (a), there appears to be an additional hydrogen bond interaction between the methyl hydrogen and the carbonyl oxygen, as well as one between the methoxy oxygen and a maleimide  $\alpha$ -hydrogen. A similar analysis previously made for the reaction of the ether **2** with maleic anhydride used a smaller basis set than the one used here.<sup>4</sup> In order to directly compare this, the minimum Gibbs energy and Gibbs energy of activation of ether **2** with maleic



**FIGURE 2.** (Panel a) Minimum energy structure reaction geometry (a) for **5f**. (Panel b) Transition state structure reaction geometry (a) for **5f**. (Panel c) Minimum energy structure reaction geometry (f) for **5f**. (Panel d) Transition state structure reaction geometry (f) for **5f**.

## SCHEME 4. Diels–Alder Reaction of Carbinol 1

TABLE 3. Thermal Diels–Alder Additions of Carbinol 1 with Maleimides 4a–e<sup>a</sup>

entry	imide	solvent	conv (%) <sup>b</sup>	dr (%) <sup>b</sup>
1	<b>4a</b>	CH <sub>2</sub> Cl <sub>2</sub>	> 95	55:45
2	<b>4a</b>	toluene	> 95	63:37
3	<b>4b</b>	CH <sub>2</sub> Cl <sub>2</sub>	> 95	52:48
4	<b>4b</b>	toluene	> 95	51:49
5	<b>4c</b>	CH <sub>2</sub> Cl <sub>2</sub>	> 95	48:52
6	<b>4c</b>	toluene	> 95	47:53
7	<b>4d</b>	CH <sub>2</sub> Cl <sub>2</sub>	> 95	55:45
8	<b>4d</b>	toluene	> 95	53:47
9	<b>4e</b>	CH <sub>2</sub> Cl <sub>2</sub>	> 95	68:32
10	<b>4e</b>	toluene	> 95	64:36

<sup>a</sup>Reactions performed by heating carbinol **1** (1.7 mmol) and dienophile (1.7 mmol) in dry degassed solvent (15 mL) at reflux for 2 h, followed by evaporation of the solvent. <sup>b</sup>Calculated from the ratios of the integrals corresponding to appropriate signals in the <sup>1</sup>H NMR spectrum of the crude reaction mixture.

anhydride were calculated to be 14 and 136.4 kJ/mol, respectively, compared to 22.2 and 145.0 kJ/mol, respectively, compared to the smaller basis set. It is likely then that the previously adopted methodology is most likely overestimating the Gibbs energy for this reaction.

Similar studies were conducted for the thermal Diels–Alder reactions of the alcohol **1** with maleimides **4a–e** by heating at reflux in dry degassed solvent for 2 h (Scheme 4). All cycloadditions proceeded with complete conversion, and the addition products **6a–e** and **7a–e** were found to precipitate from the reaction mixture on cooling. The reaction of *tert*-butylmaleimide **4c** was significantly faster with the carbinol **1** than with the corresponding methyl ether **2** under the same reaction conditions (entry 5, Table 3). This result is also in agreement with previous studies where *N*-methylmaleimide reacted more quickly with alcohol **1** than with ether **2** when refluxed in various solvents (toluene, xylene, mesitylene).<sup>3d</sup> As expected from previous studies, formation of two diastereomeric products were observed in all cases and no effect on the product distribution was observed by increasing the reflux temperature by changing solvent from CH<sub>2</sub>Cl<sub>2</sub> to toluene and/or extending the reaction time to 4 h. Attempts to separate the resulting diastereoisomers by either flash column chromatography or fractional crystallization proved to be difficult, thus making the characterization as a mixture necessary.

The relative diastereomeric ratios of approximately 1:1 mixtures in all the cases indicated that the *N*-substituent on the maleimide appeared to have no significant effect in the selectivity of these reactions, the only exception perhaps

TABLE 4. Gibbs Energy of Formation and Gibbs Energy of Activation Compared to Reactants at Infinite Separation for the 6 Reaction Geometries in the Formation of **6f** [(a)–(c)]/**7f** [(d)–(f)] Depicted in Figure 1 (X = H)

reaction geometries	Gibbs energy of activation (kJ/mol)	Gibbs energy of reaction (kJ/mol)
(a)	138.01	4.73
(b)	153.03	−0.40
(c)	164.62	28.90
(d)	134.02	9.12
(e)	170.01	28.16
(f)	155.33	7.00

being with the *p*-nitro-maleimide **4e**. Unfortunately, direct evidence could not be obtained to confirm the identity of the diastereoisomers by *O*-methylation of the resulting diastereomeric mixtures and subsequent correlation with the analogous methylated cycloadducts, since extensive decomposition was obtained in all cases. However, the identity of a mixture of cycloadducts (37:63 ratio) from the cycloaddition of the *N*-methylmaleimide to carbinol **1** has been previously confirmed by Snyder and co-workers.<sup>2a</sup> A comparison of the chemical shift difference from the <sup>1</sup>H NMR spectra of the cycloadducts **6a–e** and **7a–e** was made with the available data for the *N*-methylmaleimide *anti*-diastereoisomer **6f** and *syn*-**7f**.<sup>2a</sup> Although slight differences in chemical shifts were observed, some correlation was possible implying that the major diastereoisomers produced from the reaction with maleimides **4a** and **4e** were **6a** and **6e**, respectively, due to the better correlation to the *anti*-diastereoisomer **6f**. For reactions with maleimides **4b–d**, the levels of diastereoselectivity are too small to be meaningful, although a slight preference for the *syn*-diastereoisomer may be inferred for maleimide **4c**. The increased amount of *anti*-diastereoisomer **6e** observed with the *p*-nitrophenyl substituent (64:36 ratio) could be a consequence of the electron-withdrawing effects of the nitro group, as this could partially remove electron density from the carbonyl group and result in a poorer hydrogen bond stabilization interaction with more pronounced electrostatic repulsion, thus leading to *anti*-diastereoisomer **6e**. Again, to rationalize these results and in light of the excellent predictions for the stereochemistry of the formation of imide **5f**, a series of calculations were performed for the formation of **6f** and **7f** using DFT. Six reaction geometries were considered (Figure 1, X = H), and both the Gibbs energy of formation from reactants and the Gibbs energy for the transition state were calculated (Table 4).

The situation for imides **6f** and **7f** is more complicated than that for the ether **2**. In this case there is only one lowest energy isomer (b), but this does not have the lowest energy transition state. Thus, two additional, higher energy isomers [(a) and (d)], which have higher energies of formation but lower transition state energies, must also be considered. In the global minimum structure (Figure 3, panel a) the hydroxyl group is located below the carbonyl oxygen of the imide. In this arrangement, the hydroxyl-hydrogen atom coordinates to the carbonyl oxygen, while the oxygen coordinates to an aromatic hydrogen of the aromatic ring. The other two groups on the auxiliary do not appear to be involved in any binding interactions, and the methyl has a repulsive interaction with the hydrogen on the *N*-methylmaleimide. This repulsive interaction would appear to be the reason that the transition state for reaction geometry (b) is much higher

(4) Çelebi-Ölçüm, N.; Sanyal, A.; Aviyente, V. *J. Org. Chem.* **2009**, *74*, 2328–2336.



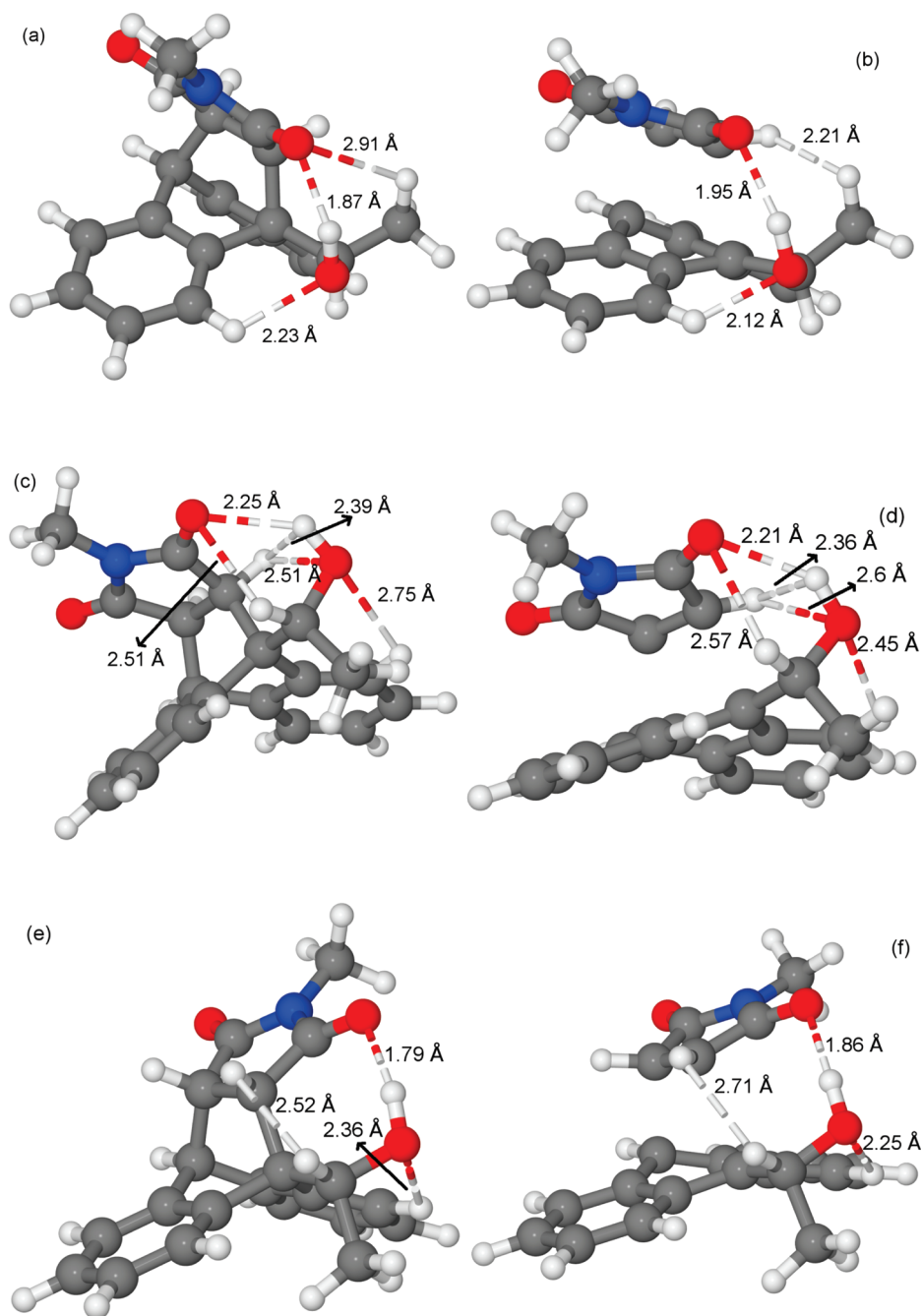
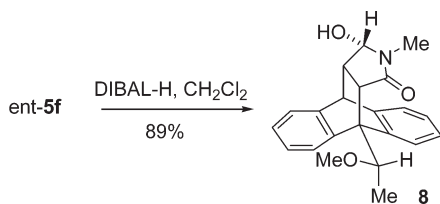


**FIGURE 3.** (Panel a) Minimum energy structure reaction geometry (b) for **6f/7f**. (Panel b) Transition state structure reaction geometry (b) for **6f/7f**. (Panel c) Minimum energy structure reaction geometry (a) for **6f/7f**. (Panel d) Transition state structure reaction geometry (a) for **6f/7f**. (Panel e) Minimum energy structure reaction geometry (d) for **6f/7f**. (Panel f) Transition state structure reaction geometry (d) for **6f/7f**.

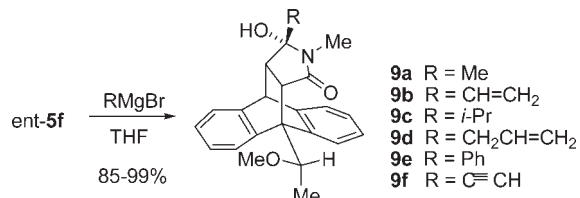
in energy than for reaction geometry (a) and (d). Reaction geometry (a) (Figure 3, panels c and d) is the equivalent of the global energy minimum for the formation of **5f**, only this time the lone hydrogen on the auxiliary is 0.4 Å further away from the carbonyl oxygen. Reaction geometry (b) also appears to have a longer hydrogen bond with the oxygen of the auxiliary. However, it is clear that the rotation of the methyl group away from the incoming maleimide has reduced its repulsive interaction, resulting in a lower transition state energy. Reaction geometry (d) (Figure 3, panels e and f) is similar to reaction geometry (b) with the hydroxyl group below the carbonyl oxygen of the maleimide. In this case in

effect the roles of the methyl and lone hydrogen have interchanged, and as a result, the transition state is lower, given that the maleimide has to pass a hydrogen atom instead of the methyl group, which is exactly what we have found. We also attempted to explain the enhanced stereoselectivity for the *p*-NO<sub>2</sub>Ph substituted maleimide. However, no definite conclusions could be drawn from these calculations regarding the stereoselectivity. The minimum energy structure appeared to be similar to that for **6f/7f**, with the van der Waals interaction between the aromatic hydrogen atoms on the *p*NO<sub>2</sub>Ph group and the carbonyl oxygen atom being the major difference with **6f/7f**.

## SCHEME 5. Selective Reduction of Imide 5f



## SCHEME 6. Selective Addition of Grignard Reagent to Imide 5f



The feasibility of performing asymmetric transformations at the carbonyl group of cycloadducts ent-5a–f using the *N*-methylmaleimide adduct ent-5f as a model substrate were next considered.<sup>5</sup> Carbonyl reduction using Superhydride (LiEt<sub>3</sub>BH) resulted in recovery of starting material, although it was reported to give a clean reduction with the structurally similar *N*-alkylmaleimide cycloadducts.<sup>2d</sup> Lithium aluminum hydride was capricious in its reactivity; however, reduction with DIBAL-H furnished hydroxy lactam 5f in high yield and with excellent regio- and diastereoselectivity, occurring solely at the carbonyl remote to the original C9 anthracene substituent (Scheme 5).

The regioselectivity was confirmed from multiplicity of the bridgehead signals at 2.76 and 4.86 ppm in the <sup>1</sup>H NMR spectrum of the reduced cycloadduct 8. The facial selectivity was confirmed by examining the coupling constant of the hydroxy-lactam proton ( $J_{\text{obs}}$  7.9 Hz), which correlates better with the predicted magnitude of coupling constant for a dihedral angle for an (*S*)-configured product (1.3°,  $J_{\text{pred}}$  8–10 Hz) than for the (*R*) case (124.3°,  $J_{\text{pred}}$  1–2 Hz). Similarly, Grignard additions to cycloadduct 5f also occurred solely at the remote carbonyl and produced the corresponding hydroxy-lactams 9a–f in excellent yields and selectivity, varying from 85% to 99% without any need for purification (Scheme 6, Table 5).

As described earlier, <sup>1</sup>H NMR spectroscopy was again used to correlate the regio- and diastereoselectivity of the transformations. In addition, single crystal X-ray analysis confirmed the stereochemistry of hydroxy-lactam 9a. The high regioselectivity observed in this process has been rationalized by the developing repulsive interactions between the auxiliary attached to C9 of anthracene and the carbonyl oxygen in the transition state that results from addition to the proximal carbonyl group, as the hybridization of the carbonyl carbon changes from sp<sup>2</sup> to sp<sup>3</sup>.<sup>2d</sup> However, such a rationalization would suggest that this reaction is reversible, an observation for which we have not found any evidence. To shed more light on this observation we have studied the Grignard reaction using DFT. A complication in such a study is that the exact form of the transition state is unknown

(5) Note that for these series of compounds, the opposite enantiomer of cycloadduct was used.

TABLE 5. Yields from Addition of Grignard Reagents to Imide 5f<sup>a</sup>

entry	product	yield (%) <sup>b</sup>
1	9a	91
2	9b	97
3	9c	85
4	9d	87
5	9e	86
6	9f	89

<sup>a</sup>Reactions performed by adding the appropriate quantity of a solution of Grignard reagent to imide 5f (1.7 mmol) in dry degassed THF (12 mL) at 0 °C under a nitrogen atmosphere. The solution was left for 30 min and then allowed to warm to rt for 18 h, before standard workup followed by evaporation of the solvent. <sup>b</sup>Based on isolated product.

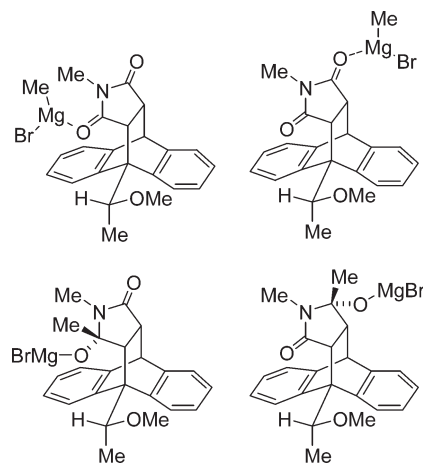
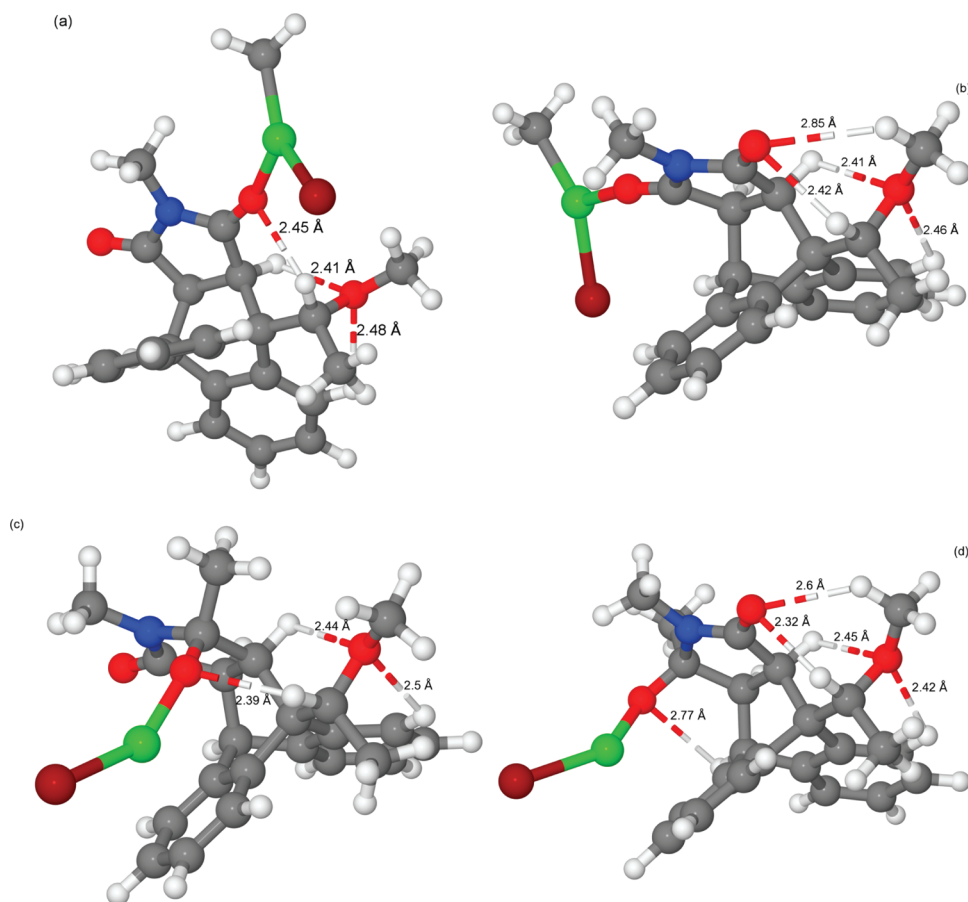


FIGURE 4. Precoordinated structures and addition products modeled for the addition of MeMgBr to maleimide 5f.

and therefore not amenable to theoretical treatment. Although a stepwise ionic mechanism is conventionally drawn for the addition to a Grignard reagent of a carbonyl group, in practice there is evidence to support a radical-like process.<sup>6</sup> For this exercise, we sought to model the formation of an initial pre-coordinated Grignard reagent, as well as the energy of the final product from the transformation (Figure 4).

Comparing the pre-reaction complexes (Figure 5a and b), it is clear that the main difference between the two is the fact that in the complex where addition occurs proximal to the stereogenic center, the hydrogen bond between the carbonyl oxygen and the methoxy-hydrogen is broken and the methyl group rotates away from the steric bulk of the complex. Moreover, there are no obvious interactions which may compensate for the loss of this van der Waals bond. In the case of addition to the carbonyl group distal to the stereogenic center, there is no need for this hydrogen bond to break. In addition, the bromine on the MeMgBr can coordinate to the H-10 hydrogen atom of the cycloadduct. As a consequence, it is no surprise that the Gibbs energy of the distal complex is 7.1 kJ/mol lower than that of the proximal complex. If this is indeed the determining step for the regioselectivity of the Grignard reaction, then assuming Boltzmann statistics, this would lead to a 93:7 ratio in favor of the distal complex, in excellent agreement with the experimental data.

(6) Maruyama, K.; Katagiri, T. *J. Phys. Org. Chem.* **1989**, 2, 205–213.

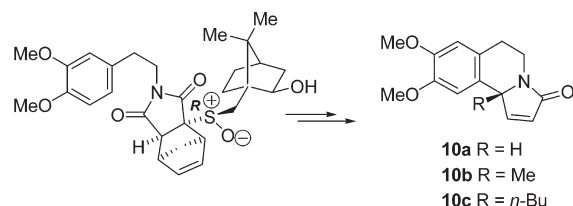


**FIGURE 5.** Four different structures for Grignard reaction. (a) Complex proximal. (b) Complex distal. (c) Product proximal. (d) Product distal.

The relative energetics are very similar for the products formed from the two complexes (Figure 5c and d). As a result, the Gibbs energy of the distal product is 11.5 kJ/mol lower than that of the proximal product. It is worth noting here that in both cases there is a significant interaction between the magnesium atom and the  $\pi$ -system of the anthracene moiety. This interaction has been found before to be important in the structure of zinc-based complexes.<sup>7</sup> Also, the distal product again introduces a hydrogen bond, this time between the H-10 hydrogen atom of the cycloadduct and the distal alkoxy substituent.

Having established excellent regio- and stereoselectivity, studies were directed toward using this methodology in the synthesis of the pyrrolo[2,1-*a*]isoquinoline framework, which represents a structural fragment of erythrinan alkaloids that have been shown to elicit significant pharmacological activity.<sup>8</sup> Pyrrolo[2,1-*a*]isoquinolines **10a–c** have been previously accessed by employing a similar chiral diene strategy that used a chiral sulfoxide to control the diastereoselectivity of the Diels–Alder reaction and ensuing transformations.<sup>9</sup>

#### SCHEME 7. Synthesis of Pyrrolo[2,1-*a*]isoquinolines



However, the chiral diene was not recyclable, since the sulfoxide needed was removed before the final retro-Diels–Alder reaction (Scheme 7).

In the case of the product **10a**, reduction of the alkene and carbonyl group would provide us with an efficient route to prepare the antitumor alkaloid crispine **A**<sup>10</sup> in an enantiomerically pure form, circumventing any issues relating to *endo/exo* selectivity in the Diels–Alder reaction, in addition to allowing for efficient recycling of the auxiliary.

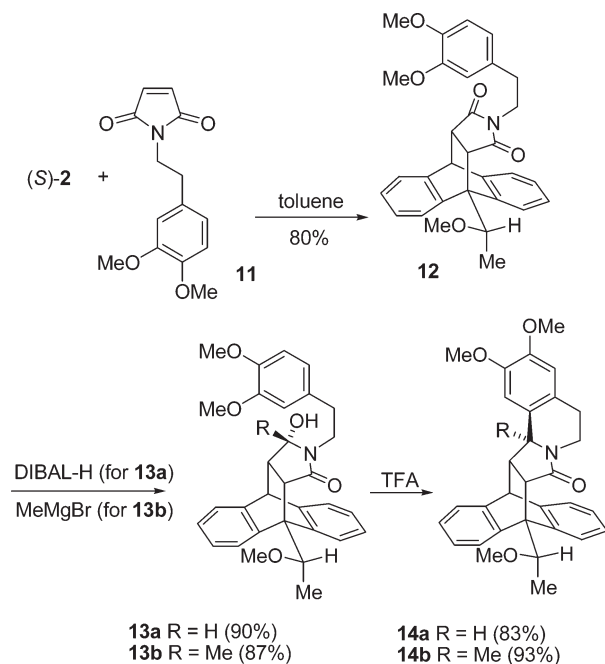
*N*-[2-(3,4-Dimethoxyphenyl)ethyl]maleimide **11** was accessed in good yield (78%) from commercially available 2-(3,4-dimethoxyphenyl)ethylamine and maleic anhydride following a previously reported procedure.<sup>9b</sup> Thermal Diels–Alder reaction of this with the enantiomerically pure methyl ether (*S*)-**2** was carried out by heating at reflux in toluene for 2 h, affording the addition product **12** as single

(7) Dreiocker, F.; Oomens, J.; Meijer, A. J. H. M.; Pickup, B. T.; Jackson, R. F. W.; Schäfer, M. *J. Org. Chem.* **2010**, *75*, 1203–1213.

(8) Mikhailovskii, A. G.; Shklyayev, V. S. *Chem. Heterocycl. Compd. (N. Y., NY, U. S.)* **1997**, *33*, 243–265.

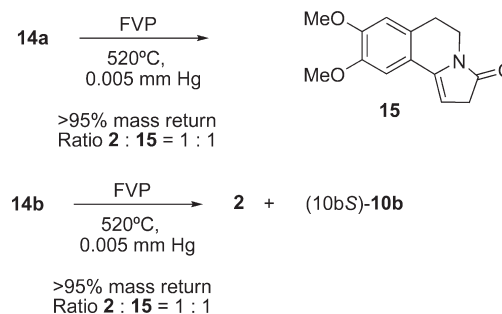
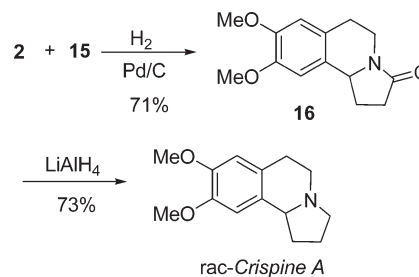
(9) (a) Collado, M. I.; Manteca, I.; Sotomayor, N.; Villa, M.-J.; Lete, E. *J. Org. Chem.* **1997**, *62*, 2080–2092. (b) Manteca, I.; Etxarri, B.; Ardeo, A.; Arrasate, S.; Osante, I.; Sotomayor, N.; Lete, E. *Tetrahedron* **1998**, *54*, 12361–12378. (c) Gonzalez-Temprano, I.; Osante, I.; Lete, E.; Sotomayor, N. *J. Org. Chem.* **2004**, *69*, 3875–3885.

(10) Coldham, I.; Jana, S.; Watson, L.; Martin, N. G. *Org. Biomol. Chem.* **2009**, *7*, 1674–1679 and references therein.

**SCHEME 8. Preparation of Friedel–Crafts Products 14a and 14b**


diastereoisomer, which after flash column chromatography was isolated in good yield (Scheme 8). In line with previous results and correlation of the NMR data, the sense of the diastereoselectivity for this cycloaddition was consistent with the other maleimide analogues **5a–e**. Reduction of cycloadduct **12** with DIBAL-H provided hydroxy-lactam **13a** as single diastereoisomer in quantitative yield, unsurprisingly following the expected pattern of diastereo- and regioselectivity observed with other substrates. Similarly, addition of MeMgBr afforded hydroxy-lactam **13b** in excellent yield. Subsequent intramolecular Friedel–Crafts reaction of hydroxy-lactams **13a** and **13b** with an excess TFA afforded methaneisoindoloisoquinolines **14a** and **14b** in good yields after purification by flash column chromatography. The relative stereochemistry of compound **14a** was confirmed by single crystal X-ray diffraction, which clearly showed the hydrogen atom attached to the (*S*)-configured stereogenic center at C-14b and indicated that reaction proceeded via addition to the least hindered *re* face of the *N*-acyl iminium ion generated during the reaction.

A retro-Diels–Alder reaction was performed on amides **14a** and **14b** utilizing flash vacuum pyrolysis (FVP) at 520 °C, 0.005 mmHg, in each case leading to high conversion to a 1:1 mixture of auxiliary and product (Scheme 9). In each case the yield of the recovered auxiliary **2** was high and in excellent enantiomeric excess. Whereas the product obtained from the retro-Diels–Alder reaction of amide **14b** was the expected  $\alpha,\beta$ -unsaturated amide **10b** (isolated in high yield and enantiomeric excess), the product using substrate **14a** was the unexpected achiral isomer **15**. Clearly a retro-Diels–Alder reaction had occurred, but rapid isomerization of the product to the more thermodynamically stable alkene ensued. Attempts to purify this compound by silica gel chromatography led to decomposition, presumably through hydrolysis of the enamide. Similar observations with regard to decomposition of the FVP product have been made with

**SCHEME 9. Flash Vacuum Pyrolysis of Amides 14a and 14b**

**SCHEME 10. Synthesis of *rac*-Crispine A**


related studies upon chiral sulfoxide dienes, although the identity of the FVP product was not established.<sup>9c</sup>

Hydrogenation of the mixture of enamide **15** and ether **2** gave lactam **16** in quantitative yield after separation and recovery of ether **2**. Lithium aluminum hydride reduction afforded crispine A in good yield (Scheme 10). Naturally, in light of the isomerization to enamide **15**, the product was racemic as confirmed by comparison of the value of the optical rotation and HPLC analysis.

In conclusion, we have demonstrated that ether **2** can function as an effective chiral auxiliary, allowing efficient recovery and recycling without no loss of enantiomeric excess. The selectivity of Diels–Alder reactions of the ether **2** with maleimides is independent of the electronic and steric effects of the group attached to nitrogen, although small differences are seen with the corresponding alcohol **1**. Highly regio- and diastereoselective transformations are possible with a variety of nucleophilic reagents, and the resultant hydroxy-lactams permit further stereoselective transformations, including Friedel–Crafts reactions. One limitation of the methodology is the susceptibility of any retro-Diels–Alder product to undergo racemisation should an acidic proton be located in the  $\gamma$ -position, a necessary consideration when appraising the potential of this strategy toward a synthetic target.

**Experimental Section**

**(*R*)-1-Anthracen-9-yl Ethanol 1.** B(OMe)<sub>3</sub> (0.20 cm<sup>3</sup>, 1.8 mmol) was added to a solution of *cis*-(1*S*,2*R*)-1-aminoindan-2-ol (0.20 g, 1.4 mmol) in THF (1 mL) and stirred at rt for 30 min. BH<sub>3</sub>·DMS complex (1.20 mL, 12.5 mmol) in THF (1 mL) was added, and the resulting solution cooled to 0 °C before addition of 1-anthracen-9-yl ethanone **3**<sup>3d</sup> (2.50 g, 11.4 mmol) in THF (3.50 mL). The reaction mixture was stirred for 2.5 h at 0 °C, quenched with MeOH (10 mL), and allowed to warm to rt. H<sub>2</sub>O was added (10 mL), and the product was extracted into CH<sub>2</sub>Cl<sub>2</sub> (3 × 10 mL), washed with (1 M aq) HCl (10 mL) and



H<sub>2</sub>O (10 mL) and dried over MgSO<sub>4</sub>. Removal of the solvent gave the title compound **1** (2.54 g, > 99%, ee 81%) as a yellow solid. Repeated recrystallization from CH<sub>2</sub>Cl<sub>2</sub> and petroleum ether 40–60 °C afforded **1** (0.73 g, 44%, ee > 99%) as yellow crystals confirmed by comparison of the NMR data with the literature;<sup>3d</sup> [ $\alpha$ ]<sub>D</sub><sup>25</sup> +18.5 (*c* 1, CHCl<sub>3</sub>; ee > 99%) [lit.<sup>3d</sup> –17.5 (*c* 1, CHCl<sub>3</sub>; ee 96% for (*S*)-enantiomer)]; mp 112–114 °C (lit.<sup>3d</sup> 116–117 °C); CSP HPLC (Chiracel OD, 1.0 mL/min, 95:5 hexanes/*i*-PrOH); *t*<sub>R</sub> 25.4 and 55.6 min.

**General Procedure A for the Thermal Diels–Alder Cycloaddition of 9-Anthryl Derivative Compounds 1 or 2 to Maleimide Derivatives 4a–e.** A solution of anthryl derivative **1** or **2** (prepared by an established literature method<sup>3d</sup>) (1.7 mmol) and maleimides **4a–e** (either commercially available or prepared by an established literature method<sup>11</sup>) (1.7 mmol) in dry degassed solvent (15 mL) was heated at reflux for 2 h and sampled as appropriate. Removal of the solvent produced the desired cycloadduct (conversion calculated from <sup>1</sup>H NMR spectrum).

**(3aR,9aR)-3a,4,9,9a-Tetrahydro-4-[(1R)-1-methoxyethyl]-2-hydroxy-4,9-[1',2']benzeno-1H-benzof[*f*]isoindole-1,3-(2H)-dione 5a.** Obtained as white crystals in 86% yield using general procedure A by heating (*R*)-9-(1-methoxyethyl)anthracene **2** with maleimide **4a** followed by recrystallization from CH<sub>2</sub>Cl<sub>2</sub>/petrol 60–80 °C: mp 255–257 °C (from CH<sub>2</sub>Cl<sub>2</sub>/petrol 60–80 °C) [lit.<sup>2a</sup> 270–272 °C (racemic) from EtOAc/hexanes]; [ $\alpha$ ]<sub>D</sub><sup>22</sup> –69.0 (*c* 1, CHCl<sub>3</sub>); IR (ATR) 1769, 1716, 1697 cm<sup>–1</sup>; <sup>1</sup>H NMR (300 MHz; CDCl<sub>3</sub>)  $\delta$  1.88 (d, *J* = 6.3 Hz, 3H), 3.18 (dd, *J* = 3.2, 8.6 Hz, 1H), 3.68 (d, *J* = 8.6 Hz, 1H), 3.71 (s, 3H), 4.72 (d, *J* = 3.2 Hz, 1H), 5.10 (q, *J* = 6.3 Hz, 1H), 7.18–7.22 (m, 5H), 7.33–7.40 (m, 3H), 7.84–7.90 (m, 1H); <sup>13</sup>C NMR (125 MHz, CDCl<sub>3</sub>)  $\delta$  16.6, 46.1, 47.9, 49.8, 54.4, 56.9, 73.5, 123.7, 125.2, 125.8, 126.3, 126.6, 126.7, 126.8, 138.2, 138.7, 139.1, 142.3, 175.9, 176.4; HRMS (EI<sup>+</sup>) calcd for C<sub>21</sub>H<sub>19</sub>NO<sub>3</sub> (M<sup>+</sup>) 333.1365, found 333.1376. Anal. Calcd for C<sub>21</sub>H<sub>19</sub>NO<sub>3</sub>: C, 75.66; H, 5.74; N, 4.20. Found: C, 75.39; H, 5.64; N, 4.12.

**(3aS,9aS)-3a,4,9,9a-Tetrahydro-4-[(1S)-1-hydroxyethyl]-2-hydroxy-4,9-[1',2']benzeno-1H-benzof[*f*]isoindole-1,3-(2H)-dione 6a and (3aR,S,9aR,S)-3a,4,9,9a-Tetrahydro-4-[(1S)-1-hydroxyethyl]-2-hydroxy-4,9-[1',2']benzeno-1H-benzof[*f*]isoindole-1,3-(2H)-dione 7a.** Obtained as white powder in quantitative yield as a 63:37 ratio (55:45 in CH<sub>2</sub>Cl<sub>2</sub>) of **6a**:**7a** using general procedure A by heating ( $\pm$ )-1-anthracen-9-yl ethanol **1** with maleimide **4a** in dry toluene. The diastereoisomers were inseparable by flash column chromatography and were characterized as a mixture (60:40 ratio): mp 282–284 °C (from CH<sub>2</sub>Cl<sub>2</sub>/petrol 40–60 °C); IR (ATR) 3531, 3336, 1782, 1716 cm<sup>–1</sup>; <sup>1</sup>H NMR (250 MHz, DMSO)  $\delta$  major diastereoisomer 1.77 (d, *J* = 6.1 Hz, 3H), 3.10 (dd, *J* = 3.1, 8.6 Hz), 3.52 (d, *J* = 8.6 Hz, 1H), 4.64 (d, *J* = 3.1, 1H), 5.41–5.49 (m, 2H), 7.09–7.30 (m, 6H, m), 7.42–7.45 (m, 1H), 7.94–7.97 (m, 1H), 10.64 (s, 1H); minor diastereoisomer 1.80 (d, *J* = 6.1 Hz, 3H), 3.18 (d, *J* = 8.8 Hz, 1H), 3.24 (dd, *J* = 2.9, 8.8 Hz, 1H), 4.61 (d, *J* = 2.9 Hz, 1H), 5.32–5.35 (m, 2H), 7.09–7.30 (m, 5H), 7.42–7.44 (m, 1H), 7.57 (d, *J* = 6.7 Hz, 1H), 7.93–7.96 (m, 1H), 10.74 (s, 1H); <sup>13</sup>C NMR (65 MHz, DMSO)  $\delta$  major diastereoisomer 21.6, 45.8, 48.1, 50.0, 54.2, 65.0, 118.9, 124.3, 124.5, 125.3, 125.6, 126.3, 126.7, 127.2, 140.1, 141.8, 144.0, 177.7, 178.2; minor diastereoisomer 20.8, 45.2, 48.6, 49.7, 52.5, 63.6, 124.3, 124.5, 124.6, 124.9, 125.6, 125.9, 126.2, 127.1, 139.7, 140.4, 141.1, 143.8, 177.7, 178.3; HRMS (TOF ES<sup>+</sup>) calcd for C<sub>20</sub>H<sub>18</sub>NO<sub>3</sub> (MH<sup>+</sup>) 320.1287, found 320.1276.

**(3aS,9aS,3S)-3a,4,9,9a-Tetrahydro-4-[(1S)-1-methoxyethyl]-3-hydroxy-2-methyl-4,9-[1',2']benzeno-1H-benzof[*f*]isoindole-1-(1H)-one 8.** DIBAL-H 1 M in hexane (0.60 mL, 0.58 mmol) was added dropwise to a stirred solution of cycloadduct ent-**5f** (0.10 g, 0.29 mmol) in CH<sub>2</sub>Cl<sub>2</sub> (5 mL) at –78 °C. The reaction mixture

was stirred for 2.5 h at –78 °C, then quenched with 1 M HCl (7 mL), and allowed to warm to rt, and H<sub>2</sub>O (10 mL) was added. After 15 min of stirring, the product was extracted into CH<sub>2</sub>Cl<sub>2</sub> (3  $\times$  10 mL) and dried over MgSO<sub>4</sub>, and the solvent was removed *in vacuo* to produce the hydroxy-lactam **8** as a white powder that was pure enough to be used in any subsequent transformations without purification (0.09 g, 89%). The hydroxy-lactam was purified *via* recrystallization from CH<sub>2</sub>Cl<sub>2</sub>/petroleum ether 60–80 °C for characterization purposes as white crystals: [ $\alpha$ ]<sub>D</sub><sup>25</sup> –31.0 (*c* 1, CHCl<sub>3</sub>); mp 197–199 °C; IR (thin film) 3386, 2925, 1652, 1456 cm<sup>–1</sup>; <sup>1</sup>H NMR (400 MHz; CDCl<sub>3</sub>)  $\delta$  1.87 (d, *J* = 6.4 Hz, 3H), 2.42 (d, *J* = 12.0 Hz, 1H), 2.49 (s, 3H), 2.84 (ddd, *J* = 2.3, 8.1, 10.0 Hz, 1H), 3.47 (d, *J* = 10.0 Hz, 1H), 3.74 (3H, s, OCH<sub>3</sub>), 4.66 (d, *J* = 2.3 Hz, 1H), 4.95 (dd, *J* = 8.1, 12.0 Hz, 1H), 5.43 (q, *J* = 6.4, 1H), 7.15–7.22 (m, 4H), 7.28–7.35 (m, 2H), 7.41–7.43 (m, 1H), 7.87–7.89 (m, 1H); <sup>13</sup>C NMR (100 MHz; CDCl<sub>3</sub>)  $\delta$  17.1, 26.7, 44.0, 45.0, 48.8, 54.8, 57.2, 73.9, 84.0, 123.3, 124.1, 124.9, 125.6, 126.0, 126.4, 126.8, 140.3, 141.2, 141.3, 144.0, 171.7; HRMS (EI) calcd for C<sub>22</sub>H<sub>23</sub>NO<sub>3</sub> (M<sup>+</sup>) 349.1678, found 349.16923. Anal. Calcd for C<sub>22</sub>H<sub>23</sub>NO<sub>3</sub>: C, 75.62; H, 6.63; N, 4.01. Found: C, 75.58; H, 6.60; N, 3.82.

**General Procedure B for the Grignard Addition to Cycloadduct ent-5f.** A solution of Grignard reagent (1.2–5 equiv) was added dropwise *via* syringe to a stirred solution of the cycloadduct ent-**5f** (0.58 mmol) in degassed THF (15 mL) at 0 °C under N<sub>2</sub>. The solution was stirred for 0.5 h at 0 °C, and then the mixture was allowed to warm to rt and stirred for a further 18 h. The reaction was quenched by the addition of saturated aqueous NH<sub>4</sub>Cl (10 mL). After 15 min of stirring at rt, the mixture was extracted with CH<sub>2</sub>Cl<sub>2</sub> (3  $\times$  20 mL), the combined organic layers were dried over MgSO<sub>4</sub> and filtered, and the solvent was removed *in vacuo* to afford the desired Grignard addition products. Purification was carried out as appropriate.

**(3aS,9aS,3S)-3a,4,9,9a-Tetrahydro-4-[(1S)-1-methoxyethyl]-2,3-dimethyl-3-hydroxy-4,9-[1',2']benzeno-1H-benzof[*f*]isoindole-1-(1H)-one 9a.** Using general procedure B by the addition of the MeMgBr (3 M in THF, 0.25 mL, 1.2 equiv) to imide ent-**5f** (0.20 g, 0.58 mmol), the title compound **9a** was obtained after recrystallization from CH<sub>2</sub>Cl<sub>2</sub>/hexane as white crystals (0.10 g, 91%): [ $\alpha$ ]<sub>D</sub><sup>25</sup> –22.0 (*c* 1, CHCl<sub>3</sub>); mp 219–221 °C; IR (thin film) 3290, 2939, 2816, 1652, 1457 cm<sup>–1</sup>; <sup>1</sup>H NMR (400 MHz; CDCl<sub>3</sub>)  $\delta$  1.35 (d, *J* = 1.0 Hz, 3H), 1.87 (d, *J* = 6.4 Hz, 3H), 2.28 (d, *J* = 1.0 Hz, 1H), 2.39 (s, 3H), 2.63 (dd, *J* = 2.5, 10.0 Hz, 1H), 3.54 (d, *J* = 10.0, 1H), 3.73 (s, 3H), 4.64 (d, *J* = 2.5 Hz, 1H), 5.47 (q, *J* = 6.4 Hz, 1H), 7.14–7.24 (m, 4H), 7.30–7.42 (m, 3H), 7.86–7.89 (m, 1H); <sup>13</sup>C NMR (63 MHz; CDCl<sub>3</sub>)  $\delta$  17.0, 23.6, 27.3, 45.6, 48.4, 50.9, 54.9, 57.2, 73.9, 88.3, 123.3, 123.9, 125.1, 125.6, 126.0, 126.5, 126.8, 140.1, 140.5, 141.4, 143.9, 171.0; HRMS (EI) calcd for C<sub>23</sub>H<sub>25</sub>NO<sub>3</sub> (M<sup>+</sup>) 363.1834, found 363.1835. Anal. Calcd for C<sub>23</sub>H<sub>25</sub>NO<sub>3</sub>: C, 76.01; H, 6.93; N, 3.85; N, 4.01. Found: C, 75.72; H, 6.99; N, 3.71.

**(3aS,9aS)-3a,4,9,9a-Tetrahydro-4-[(1S)-1-methoxyethyl]-2-[2-(3,4-dimethoxy phenyl)ethyl]-4,9-[1',2']benzeno-1H-benzof[*f*]isoindole-1,3-(2H)-dione 12.** Obtained using general procedure A by heating at reflux a solution of (*S*)-9-(1-methoxyethyl)anthracene **2** (0.52 g, 2.2 mmol) and *N*-[2-(3,4-dimethoxyphenyl)ethyl]maleimide **11**<sup>9b</sup> (0.57 g, 2.2 mmol) in toluene to produce the cycloadduct **12** as a single diastereoisomer (0.87 g, 80%) as white crystals after recrystallization from CH<sub>2</sub>Cl<sub>2</sub>/petrol 60–80 °C: [ $\alpha$ ]<sub>D</sub><sup>25</sup> +48.0 (*c* 1, CHCl<sub>3</sub>); mp 120–122 °C; IR (thin film) 2937, 1767, 1697, 1591, 1516, 1458 cm<sup>–1</sup>; <sup>1</sup>H NMR (250 MHz; CDCl<sub>3</sub>)  $\delta$  1.82–1.89 (m, 5H), 3.11 (dd, *J* = 3.2, 8.4 Hz, 1H), 3.16–3.23 (m, 2H), 3.61 (d, *J* = 8.4 Hz, 1H), 3.73 (s, 3H), 3.82 (s, 3H), 3.84 (s, 3H), 4.74 (d, *J* = 8.4 Hz, 1H), 5.17 (q, *J* = 6.4 Hz, 1H), 6.59–6.62 (m, 2H), 6.73 (d, *J* = 7.9 Hz, 1H), 7.13–7.21 (m, 5H), 7.32–7.40 (m, 2H), 7.87–7.90 (m, 1H); <sup>13</sup>C NMR (63 MHz; CDCl<sub>3</sub>)  $\delta$  16.8, 32.7, 39.7, 46.6, 46.9, 48.7, 54.7, 55.9, 57.1, 73.8, 111.3, 111.8, 120.7, 123.7, 123.9, 125.3, 125.9, 126.4, 126.7,

(11) Kishikawa, K.; Naruse, M.; Kohmoto, S.; Yamamoto, M.; Yamaguchi, K. *J. Chem. Soc., Perkin Trans. 1* **2001**, 462–468.

126.8, 130.4, 138.6, 139.0, 139.3, 142.4, 147.5, 148.8, 176.1, 176.6; HRMS (EI) calcd for  $C_{31}H_{31}NO_5$  ( $M^+$ ) 497.2202, found 497.2195. Anal. Calcd for  $C_{31}H_{31}NO_5$ : C, 74.83; H, 6.28; N, 2.81. Found: C, 74.44; H, 6.10; N, 2.66.

**(3a*S*,9a*S*,3*S*)-3a,4,9,9a-Tetrahydro-4-[(1*S*)-1-methoxyethyl]-2-[2-(3,4-dimethoxy phenyl)ethyl]-3-hydroxy-4,9-[1',2']-benzeno-1*H*-benzo[*f*]isoindole-1-(1*H*)-one 13a.** Using general procedure **B** with imide **12** (0.20 g, 0.4 mmol) and DIBAL-H (0.80 mL, 0.80 mmol), the title compound **13a** was obtained as white crystals (0.18 g, 90%) after recrystallization from  $CH_2Cl_2$ /petrol 60–80 °C:  $[\alpha]_D -25.0$  (*c* 1,  $CHCl_3$ ); mp 170–171 °C; IR (thin film) 3391, 2936, 1655, 1516, 1458  $cm^{-1}$ ;  $^1H$  NMR (250 MHz;  $CDCl_3$ )  $\delta$  1.84 (d, *J* = 6.4 Hz, 3H), 2.12–2.24 (m, 2H), 2.35–2.47 (m, 1H), 2.78 (ddd, *J* = 2.5, 8.0, 10.0 Hz, 1H), 2.98–3.22 (m, 2H), 3.43 (d, *J* = 10.0 Hz, 1H), 3.71 (s, 3H), 3.81 (s, 6H), 4.62 (d, *J* = 2.5 Hz, 1H), 4.90 (dd, *J* = 8.0, 12.6 Hz, 1H), 5.43 (q, *J* = 6.4 Hz, 1H), 6.57–6.61 (m, 2H), 6.71 (d, *J* = 9.8 Hz, 1H), 7.11–7.20 (m, 4H), 7.28–7.33 (m, 2H), 7.38–7.41 (m, 1H), 7.83–7.87 (m, 1H);  $^{13}C$  NMR (63 MHz;  $CDCl_3$ )  $\delta$  17.0, 33.9, 42.3, 43.9, 45.0, 48.7, 54.9, 55.9, 57.2, 73.9, 83.4, 111.1, 111.7, 120.6, 123.3, 124.0, 125.1, 125.6, 126.0, 126.4, 126.8, 126.9, 131.2, 140.2, 141.2, 141.4, 143.8, 147.5, 148.8, 171.5; HRMS (EI) calcd 499.2359 for  $C_{31}H_{33}NO_5$  ( $M^+$ ), found 499.2375. Anal. Calcd for  $C_{31}H_{33}NO_5$ : 74.53; H, 6.66; N, 2.80; N, 4.01. Found: C, 74.36; H, 6.79; N, 2.69.

**(3a*S*,9a*S*,3*S*)-3a,4,9,9a-Tetrahydro-4-[(1*S*)-1-methoxyethyl]-2-[2-(3,4-dimethoxy phenyl)ethyl]-3-hydroxy-3-methyl-4,9-[1',2']-benzeno-1*H*-benzo[*f*]isoindole-1-(1*H*)-one 13b.** Using general procedure **B** by the addition of the  $MeMgBr$  (1.70 mL, 5.02 mmol) to imide **12** (0.50 g, 1.01 mmol), the title compound **13b** was obtained after recrystallization from  $CH_2Cl_2$ /hexane as white crystals (0.45 g, 87%):  $[\alpha]_D -28.0$  (*c* 1,  $CHCl_3$ ); mp 194–196 °C; IR (thin film) 3546, 3384, 2974, 2936, 1651, 1516, 1456  $cm^{-1}$ ;  $^1H$  NMR (250 MHz;  $CDCl_3$ )  $\delta$  1.31 (s, 3H), 1.75 (td, *J* = 5.1, 12.4 Hz, 1H), 1.86 (d, *J* = 6.4 Hz, 3H), 2.18 (td, *J* = 5.1, 12.4 Hz, 1H), 2.47 (s, 1H), 2.59 (dd, *J* = 2.6, 9.6 Hz, 1H), 2.76 (td, *J* = 5.1, 12.4 Hz, 1H), 3.21 (td, *J* = 5.1, 2.4 Hz, 1H), 3.51 (d, *J* = 9.6 Hz, 1H), 3.72 (s, 3H), 3.82 (s, 3H), 3.83 (s, 3H), 4.64 (d, *J* = 2.6 Hz, 1H), 5.51 (q, *J* = 6.4 Hz, 1H), 6.59–6.63 (m, 2H), 6.71–6.75 (m, 1H), 7.13–7.21 (m, 4H), 7.32–7.41 (m, 3H), 7.85–7.89 (m, 1H);  $^{13}C$  NMR (63 MHz;  $CDCl_3$ )  $\delta$  17.0, 28.3, 35.1, 41.0, 45.6, 48.1, 51.0, 55.1, 55.9, 57.3, 73.9, 88.9, 111.2, 111.8, 120.6, 123.3, 123.9, 125.2, 125.7, 126.0, 126.4, 126.9, 131.5, 139.8, 140.5, 141.5, 143.9, 147.5, 148.8, 171.1; HRMS (EI) calcd for  $C_{32}H_{35}NO_5$  ( $M^+$ ) 513.2515, found 513.2528. Anal. Calcd for  $C_{32}H_{35}NO_5$ : C, 74.83; H, 6.87; N, 2.73. Found: C, 74.60; H, 6.85; N, 2.73.

**(8a*S*,14a*S*,14b*R*)-2,3-Dimethoxy-5,6,8a,9,14,14a,14b-heptahydro-9-[(1*S*)-1-methoxyethyl]-9,14-[1',2']-benzeno-1*H*-benzo[*f*]isoindolin-[2,3-*a*]-isoquinolin-8-one 14a.** TFA (1.00 mL, 13.1 mmol) was added to a stirred solution of hydroxy-lactam **13a** (1.26 g, 2.5 mmol) in  $CH_2Cl_2$  (35 mL). The reaction mixture then refluxed for 3 h, cooled to rt, and quenched with (sat. aq)  $Na_2CO_3$  (60 mL). The resulting solution was extracted into  $CH_2Cl_2$  (3 × 60 mL), washed with brine (3 × 60 mL), and dried over  $MgSO_4$ , and the solvent was removed *in vacuo*. Recrystallization from  $CH_2Cl_2$ /petrol 60–80 °C yielded the title compound **14a** (1.01 g, 83%) as white crystals:  $[\alpha]_D -19.0$  (*c* 1,  $CHCl_3$ ); mp 227–229 °C; IR (film) 2935, 1674, 1515, 1456  $cm^{-1}$ ;  $^1H$  NMR (250 MHz,  $CDCl_3$ )  $\delta$  1.85 (d, *J* = 6.4 Hz, 3H), 2.36–2.54 (m, 2H), 2.71–2.86 (m, 2H), 3.44 (d, *J* = 10.4 Hz, 1H), 3.69 (s, 3H), 3.81 (s, 3H), 3.85–3.95 (m, 4H), 4.02 (s, 1H), 4.42 (d, *J* = 3.0 Hz, 1H), 5.29 (q, *J* = 6.4 Hz, 1H), 6.48 (s, 1H), 6.71 (s, 1H), 7.14–7.29 (m, 5H), 7.36–7.40 (m, 2H), 7.84–7.88 (m, 1H);  $^{13}C$  NMR (63 MHz,  $CDCl_3$ )  $\delta$  17.1, 27.3, 37.1, 47.6, 49.8, 50.6, 54.5, 55.9, 56.4, 57.0, 58.6, 73.5, 107.7, 111.8, 123.4, 124.1, 125.3, 125.6, 125.8, 125.9, 126.1, 126.4, 126.7, 129.8, 140.0, 140.2, 140.3, 143.7, 148.1, 170.9; HRMS (EI) calcd for  $C_{31}H_{31}NO_4$  ( $M^+$ ) 481.2253, found 481.2264.

**(8a*S*,14a*S*,14b*R*)-2,3-Dimethoxy-5,6,8a,9,14,14a-hexahydro-9-[(1*S*)-1-methoxy-ethyl]-14b-methyl-9,14-[1',2']-benzeno-1*H*-benzo[*f*]isoindolin-[2,3-*a*]-isoquinolin-8-one 14b.** TFA (0.55 mL, 7.3 mmol) was added to a stirred solution of hydroxy-lactam **13b** (0.75 g, 1.5 mmol) in  $CH_2Cl_2$  (15 mL). The reaction mixture then refluxed for 3 h, cooled to rt, and quenched with saturated aqueous  $Na_2CO_3$  (10 mL). The resulting solution was extracted into  $CH_2Cl_2$  (3 × 10 mL), washed with brine (3 × 10 mL), and dried over  $MgSO_4$ , and the solvent was removed *in vacuo*. Recrystallization from  $CH_2Cl_2$ /petrol 60–80 °C afforded the title compound **14b** (0.67 g, 93%) as white crystals:  $[\alpha]_D -48.0$  (*c* 1,  $CHCl_3$ ); mp 272–274 °C; IR (film) 2937, 1678, 1510, 1466  $cm^{-1}$ ;  $^1H$  NMR (250 MHz,  $CDCl_3$ )  $\delta$  1.59 (s, 3H), 1.84 (d, *J* = 6.4 Hz, 3H), 2.32 (dd, *J* = 3.8, 15.7 Hz, 1H), 2.72–3.04 (m, 3H), 3.42 (d, *J* = 10.1 Hz, 1H), 3.63 (s, 3H), 3.78 (s, 3H), 3.82 (s, 3H), 3.78–3.87 (m, 1H), 4.62 (d, *J* = 1.8 Hz, 1H), 5.43 (q, *J* = 6.4 Hz, 1H), 6.40 (s, 1H), 6.55 (s, 1H), 7.10–7.17 (m, 4H), 7.22–7.25 (m, 1H), 7.34–7.39 (m, 2H), 7.78–7.82 (m, 1H);  $^{13}C$  NMR (63 MHz,  $CDCl_3$ )  $\delta$  17.3, 24.9, 26.2, 35.1, 47.2, 47.6, 51.4, 54.6, 55.8, 56.4, 57.3, 61.4, 73.8, 108.6, 111.9, 122.7, 124.1, 125.3, 125.4, 125.6, 125.8, 126.0, 127.0, 136.4, 140.5, 141.5, 145.6, 147.4, 147.9, 173.8; HRMS (EI) calcd for  $C_{32}H_{33}NO_4$  ( $M^+$ ) 495.2410, found 495.2415.

**General Procedure C for the Thermal Retro-Diels–Alder Reactions Using FVP.** A 50 cm quartz thermolysis tube was connected with “O”-ring joints to a 25 mL flask containing the appropriate cycloadduct (0.3 mmol), and the other end to a liquid nitrogen cold trap. The thermolysis tube was heated at 500–520 °C under vacuum (0.01 mmHg) and the starting material was then heated to 210 °C with the help of a Kugelrohr apparatus until no more presence of cycloadduct was observed (30 min). After the system cooled to rt, the remaining residue in the trap was analyzed by  $^1H$  NMR and  $^{13}C$  NMR spectroscopy.

**(10b*S*)-8,9-Dimethoxy-10b-methyl-5,6-dihydropyrrolo[2,1-*a*]-isoquinolin-3-one 10b<sup>9c</sup>.** Obtained employing general procedure **C** using adduct **14b** (0.50 g, 1.0 mmol), trapped with a > 99% mass return as a 1:1 mixture of (*S*)-9-(1-methoxyethyl)-anthracene **2** and the title compound (10b*S*)-**10b**, respectively (100% conversion calculated from the  $^1H$  NMR spectrum). Purification by flash column chromatography on silica gel eluting with 20% to 80% EtOAc/petrol 40–60% yielded the title compound (10b*S*)-**10b** (0.23 g, 87%) as white solid;  $[\alpha]_D -225.0$  (*c* 1,  $CHCl_3$ ; ee > 99%) [lit.<sup>9c</sup> +201.4 (*c* 0.35 in  $CHCl_3$ ; ee > 99% for (*R*)-enantiomer)]; mp 145–147 °C (lit.<sup>9c</sup> 148–149 °C);  $^1H$  NMR (250 MHz,  $CDCl_3$ )  $\delta$  1.59 (s, 3H), 2.65 (dd, *J* = 4.0, 15.9 Hz, 1H), 2.92 (ddd, *J* = 6.5, 11.8, 15.9 Hz, 1H), 3.22 (ddd, *J* = 4.0, 11.8, 13.3 Hz, 1H), 3.83 (s, 3H), 3.88 (s, 3H), 4.42 (dd, *J* = 6.5, 13.3 Hz, 1H), 6.08 (d, *J* = 5.8 Hz, 1H), 6.59 (s, 1H), 6.68 (s, 1H), 7.33 (d, *J* = 5.8 Hz, 1H);  $^{13}C$  NMR (63 MHz,  $CDCl_3$ )  $\delta$  26.8, 29.2, 34.6, 55.9, 56.2, 65.5, 109.1, 112.1, 125.1, 125.3, 129.2, 147.7, 148.2, 153.2, 170.1.  $^1H$  NMR and  $^{13}C$  NMR was in accordance with the literature.<sup>9c</sup>

**8,9-Dimethoxy-5,6-dihydropyrrolo[2,1-*a*]isoquinolin-3-(2*H*)-one 15<sup>12</sup>.** Obtained employing general procedure **C** using adduct **14a** (0.10 g, 0.21 mmol), trapped with a > 99% mass return as a 1:1 mixture of (*S*)-9-(1-methoxyethyl) anthracene **2** and 8,9-dimethoxy-5,6-dihydropyrrolo[2,1-*a*]isoquinolin-3-(2*H*)-one **15**, respectively (100% conversion calculated from the  $^1H$  NMR spectrum). Due to instability of enamide **15** toward silica gel chromatography, subsequent analysis was performed on a mixture of this compound and the ether **2**: IR (film) 1698, 1610, 1510  $cm^{-1}$ ;  $^1H$  NMR (400 MHz,  $CDCl_3$ )  $\delta$  2.92 (t, *J* = 6.2 Hz, 2H), 3.27 (d, *J* = 2.7 Hz, 2H), 3.76 (t, *J* = 6.2 Hz, 2H), 3.93 (s, 3H), 3.94 (s, 3H), 5.47 (t, *J* = 2.7 Hz, 1H), 6.71 (s, 1H), 7.05 (s, 1H);  $^{13}C$  NMR (100 MHz,  $CDCl_3$ )  $\delta$  28.4, 36.9, 38.2, 56.0, 56.1, 94.6, 106.6, 110.9, 119.5, 126.8, 139.5, 148.4,

(12) Padwa, A.; Waterson, A. G. *J. Org. Chem.* **2000**, *65*, 235–244.

149.9, 176.6.  $^1\text{H}$  NMR and  $^{13}\text{C}$  NMR were in accordance with the literature.<sup>13</sup>

(±)-8,9-Dimethoxy-1,5,6,10b-tetrahydro-2H-pyrrolo[2,1-a]-isoquinolin-3-one **16**<sup>13</sup>. Pd/C (0.02 g, 10% wt) was added to a solution of a mixture of (*S*)-9-(1-methoxyethyl) anthracene **2** and isoquinoline **15** obtained by FVP (0.34 g) in anhydrous THF (22 mL) at rt. The reaction vessel was evacuated by aspirator and thoroughly purged with hydrogen (three times). The resulting heterogeneous mixture was stirred under a balloon of hydrogen for 24 h and filtered through a Celite pad, and solvent was removed *in vacuo* to give the crude compound as yellow oil. Purification by flash column chromatography on silica gel eluting with (99% EtOAc/hexane) yielded the title compound **16** (0.12 g, 71%) as a yellow oil:  $^1\text{H}$  NMR (250 MHz,  $\text{CDCl}_3$ )  $\delta$  1.78–1.92 (m, 1H), 2.42–2.72 (m, 4H), 2.83–3.08 (m, 2H), 3.87 (s, 3H), 3.88 (s, 3H), 4.28–4.36 (m, 1H), 4.74 (t,  $J = 7.7$  Hz, 1H), 6.58 (s, 1H), 6.63 (s, 1H);  $^{13}\text{C}$  NMR (100 MHz,  $\text{CDCl}_3$ )  $\delta$  28.2, 28.5, 32.2, 37.4, 56.3, 56.4, 56.9, 108.0, 111.8, 125.9, 129.8, 148.3, 148.5, 173.6.  $^1\text{H}$  NMR and  $^{13}\text{C}$  NMR were in accordance with the literature.<sup>14</sup>

(±)-8,9-Dimethoxy-1,2,3,5,6,10b-hexahydropyrrolo[2,1-a]isoquinoline (Crispine A)<sup>14</sup>. A solution of (±)-8,9-dimethoxy-1,5,6,10b-tetrahydro-2H-pyrrolo[2,1-a]isoquinolin-3-one **16** (0.13 g, 0.53 mmol) in anhydrous THF (12 mL) was added dropwise to a stirred solution of  $\text{LiAlH}_4$  (0.05 g) in anhydrous THF (12 mL) at 0 °C. The reaction mixture was heated under reflux for 3 h and then stirred for a further 15 h at rt.  $\text{Et}_2\text{O}$  (12 mL) was added before the reaction was quenched by careful addition of saturated sodium potassium tartarate in  $\text{Et}_2\text{O}$  (18 mL) and then stirred for a further 1 h before the addition of anhydrous  $\text{MgSO}_4$  prior to filtration through a Celite pad. The filtrate was evaporated under reduced pressure to give a brown oil that was purified by column chromatography using silica gel eluting with (90%  $\text{CHCl}_3/\text{MeOH}$ ) to yield a colorless solid (0.09 g, 73%); mp 87–89 °C (lit.<sup>14</sup> 88–89 °C);  $^1\text{H}$  NMR (250 MHz,  $\text{CDCl}_3$ )  $\delta$  1.70–1.81 (m, 1H), 1.85–2.03 (m, 2H), 2.33–2.41 (m, 1H),

2.63–2.80 (m, 3H), 3.00–3.13 (m, 2H), 3.18–3.23 (m, 1H), 3.53 (t,  $J = 8.1$  Hz, 1H), 3.87 (s, 6H), 6.59 (s, 1H), 6.63 (s, 1H);  $^{13}\text{C}$  NMR (100 MHz;  $\text{CDCl}_3$ )  $\delta$  22.3, 27.8, 30.6, 48.2, 53.1, 55.9, 56.0, 62.8, 108.9, 111.3, 126.1, 130.5, 147.3, 147.4; HRMS (EI) calcd for  $\text{C}_{14}\text{H}_{19}\text{NO}_2$  ( $\text{M}^+$ ) 233.1416, found 233.1406.  $^1\text{H}$  NMR and  $^{13}\text{C}$  NMR were in accordance with the literature.<sup>14</sup>

**Computational Methods.** All electronic structure calculations were performed using the SMP version of the Gaussian 09 program package (rev A2)<sup>14</sup> with the B3LYP functional method.<sup>15</sup> Gaussian was compiled using the Portland Compiler version 8.0–6 with the Gaussian-supplied version of BLAS<sup>16</sup> and ATLAS.<sup>17</sup> The 6-311G\*\* basis set was used in all calculations on all atoms.<sup>18</sup> All calculations were run *in vacuo*, in the first instance. Some calculations were repeated to take account of the effect of solvent molecules using a polarizable continuum model. The inclusion of such a solvent model did not change the conclusions we have drawn from our calculations. Therefore, these calculations will not be presented here. From the minimum energy structures for reactants and products, we generated starting points for transition state calculations using the QST3 method as implemented in Gaussian09.<sup>19</sup> All optimized structures were used in subsequent frequency calculations. All minimum energy structures found have indeed zero imaginary frequencies, whereas all transition state structures found only have a single imaginary frequency. The transition state structures were animated to double-check they corresponded to the correct transition state. The calculated harmonic frequencies were in addition used to obtain Gibbs energies at 298 K, which are reported in the main text.

**Acknowledgment.** We thank the EPSRC and the Committee of Higher Education in Libya and the Libyan People's Bureau for support. All calculations were run on the cluster of the Theoretical Chemistry Group at the University of Sheffield.

**Supporting Information Available:** Additional characterization data, copies of NMR data, and crystallographic information files in CIF format. This material is available free of charge via the Internet at <http://pubs.acs.org>.

(13) Allin, S. M.; Gaskell, S. N.; Towler, J. M. R.; Page, P. C. B.; Saha, B.; McKenzie, M. J.; Martin, W. P. *J. Org. Chem.* **2007**, *72*, 8972–8975.

(14) Frisch, M. J.; Trucks, G. W.; Schlegel, H. B.; Scuseria, G. E.; Robb, M. A.; Cheeseman, J. R.; Scalmani, G.; Barone, V.; Mennucci, B.; Petersson, G. A.; Nakatsuji, H.; Caricato, M.; Li, X.; Hratchian, H. P.; Izmaylov, A. F.; Bloino, J.; Zheng, G.; Sonnenberg, J. L.; Hada, M.; Ehara, M.; Toyota, K.; Fukuda, R.; Hasegawa, J.; Ishida, M.; Nakajima, T.; Honda, Y.; Kitao, O.; Nakai, H.; Vreven, T.; Montgomery, Jr., J. A.; Peralta, J. E.; Ogliaro, F.; Bearpark, M.; Heyd, J. J.; Brothers, E.; Kudin, K. N.; Staroverov, V. N.; Kobayashi, R.; Normand, J.; Raghavachari, K.; Rendell, A.; Burant, J. C.; Iyengar, S. S.; Tomasi, J.; Cossi, M.; Rega, N.; Millam, N. J.; Klene, M.; Knox, J. E.; Cross, J. B.; Bakken, V.; Adamo, C.; Jaramillo, J.; Gomperts, R.; Stratmann, R. E.; Yazyev, O.; Austin, A. J.; Cammi, R.; Pomelli, C.; Ochterski, J. W.; Martin, R. L.; Morokuma, K.; Zakrzewski, V. G.; Voth, G. A.; Salvador, P.; Dannenberg, J. J.; Dapprich, S.; Daniels, A. D.; Farkas, Ö.; Foresman, J. B.; Ortiz, J. V.; Cioslowski, J.; Fox, D. J. *Gaussian 09, Revision A.2*; Gaussian, Inc.: Wallingford, CT, 2009.

(15) Becke, A. D. *J. Chem. Phys.* **1993**, *98*, 5648–5652.

(16) Dongarra, J. J.; Croz, J. D.; Hammarling, S.; Duff, I. S. *ACM Trans. Math. Softw.* **1990**, *16*, 1–17.

(17) Clint Whaley, R.; Petitet, A.; Dongarra, J. J. *Parallel Computing* **2001**, *27*, 3–35. Also available as University of Tennessee LAPACK Working Note #147, UT-CS-00–448, 2000 (<http://www.netlib.org/lapack/lawns/lawn147.ps>).

(18) McLean, A. D.; Chandler, G. S. *J. Chem. Phys.* **1980**, *72*, 5639–5648.

(19) Peng, C.; Ayala, P. Y.; Schlegel, H. B.; Frisch, M. J. *J. Comput. Chem.* **1980**, *17*, 49–56.